Marine seismic source simulations, and finite differences for forward and adjoint wavefields with topography and elastic-acoustic coupling

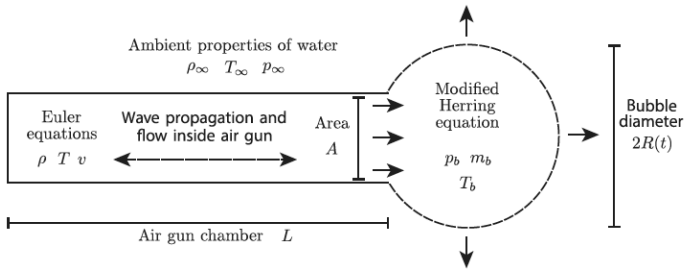

Figure 3. Schematic diagram of the coupled air-gun/bubble model.

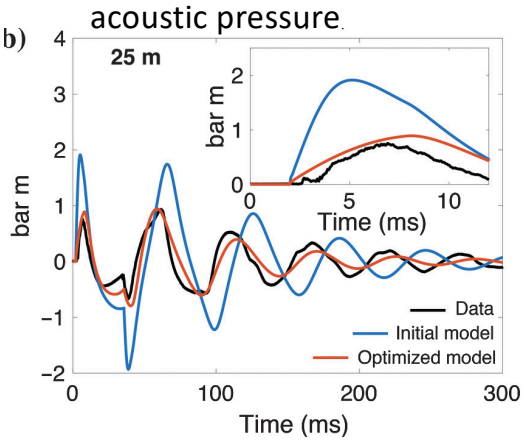

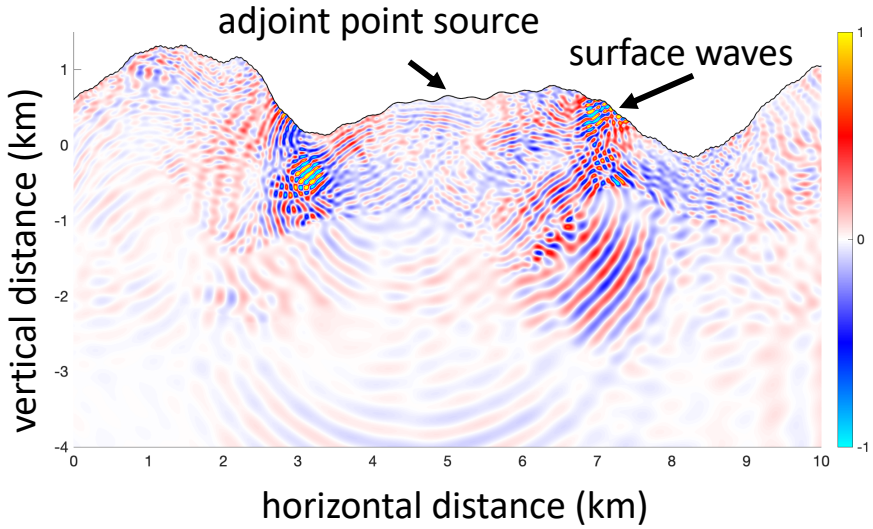

Eric M. Dunham, Stanford Geophysics

Leighton Watson, Jonatan Werpers, Shuki Ronen (on seismic sources)

Martin Almquist, Joe Jennings (on finite differences)

Complex source signature imprinted on data

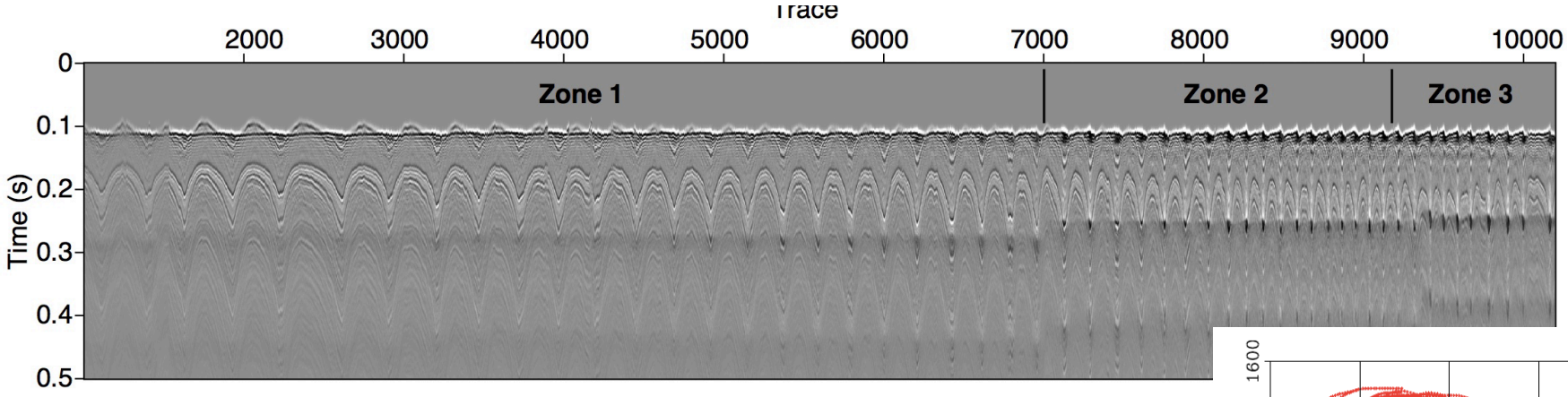

Figure 3: Data in the time domain after HMO (top) and frequency domain (bottom). Note the discontinuities around trace 7000 and trace 9300 due to the airgun failure.

source time function determined by ***oscillation dynamics of air bubbles*** released by marine seismic sources

[Watson et al., 2017]

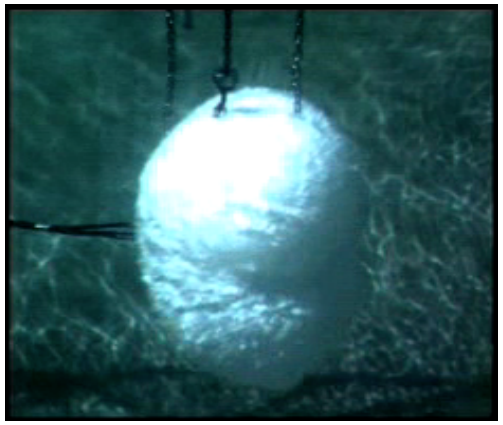

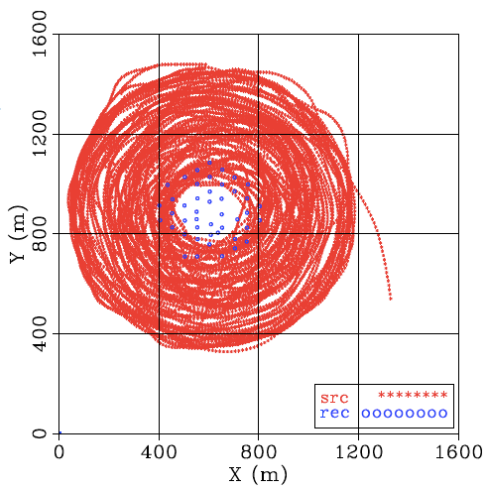

Figure 4: Shot-receiver geometry for the Apache Forties survey around the Delta platform.

Complex source signature imprinted on data

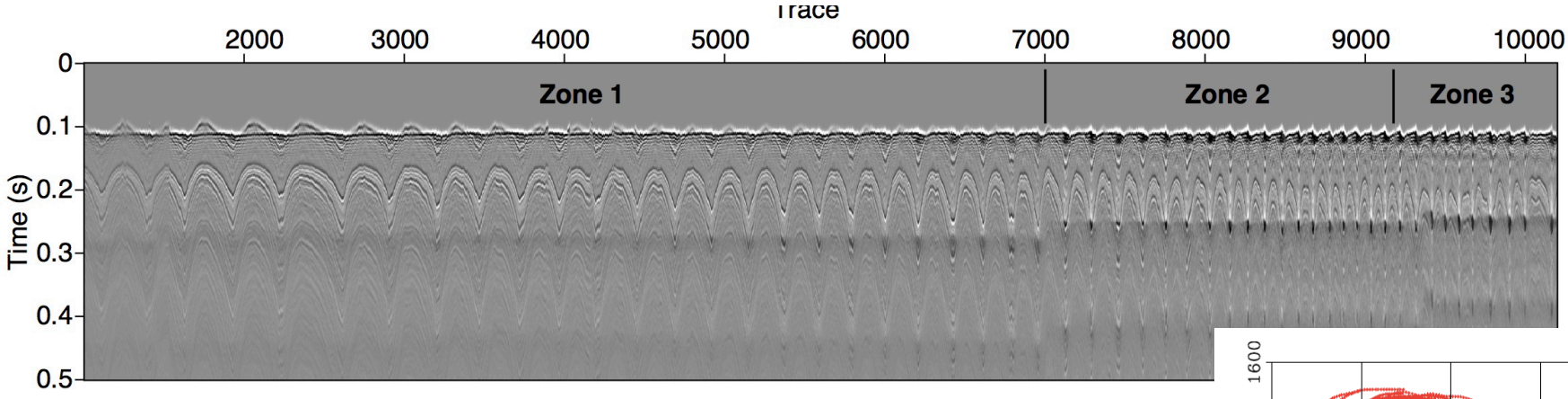

Figure 3: Data in the time domain after HMO (top) and frequency domain (bottom). Note the discontinuities around trace 7000 and trace 9300 due to the airgun failure.

one motivation: utilize ***physical modeling*** to improve source designaturing

challenging in practice because real source signatures are more complex than those from modeling

[Watson et al., 2017]

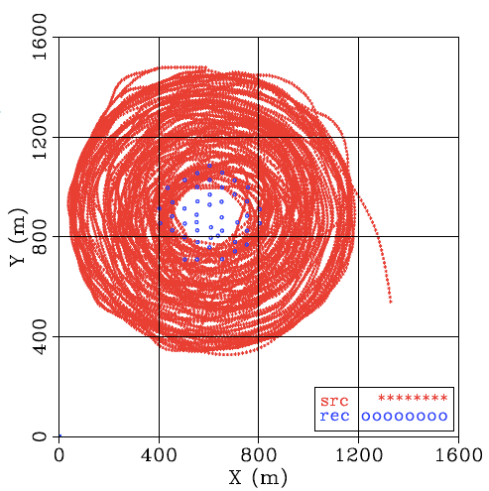

Figure 4: Shot-receiver geometry for the Apache Forties survey around the Delta platform.

Complex source signature imprinted on data

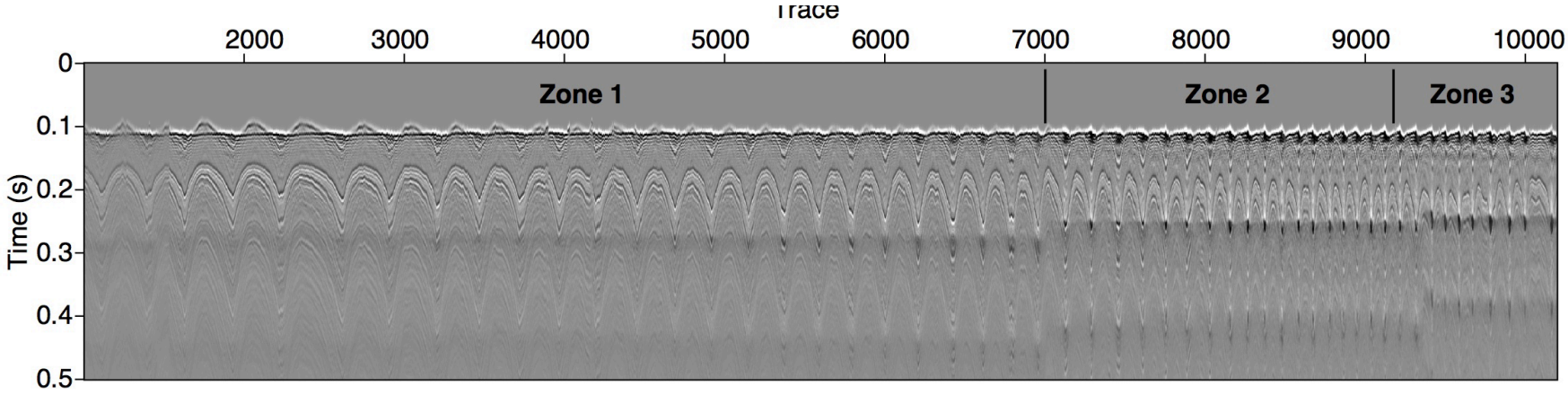

Figure 3: Data in the time domain after HMO (top) and frequency domain (bottom). Note the discontinuities around trace 7000 and trace 9300 due to the airgun failure.

one motivation: utilize ***physical modeling*** to improve source designaturing

challenging in practice because real source signatures are more complex than those from modeling

[Watson et al., 2017]

Alternatives:

- purely statistical methods like prediction error filter [Yilmaz, 2011]
- near-field hydrophones [Ziolkowski et al., 1981, 1984; Ziolkowski, 1991; Landrø et al., 1991; Landrø and Sollie, 1992; Laws et al., 1998; Hargreaves et al., 2015, 2016; Kryvohuz and Campman, 2016]

Suggestion: utilize combination of physical modeling and data (many possible approaches, such as Kalman filters)

New source designs

large volume, low pressure sources

second motivation: utilize ***physical modeling*** to improve source design

computationally efficient forward model enables optimization with various objectives:

- increase low frequencies (useful for imaging)
- decrease high frequencies (environmental issues)
- maximize radiation efficiency = acoustic energy / work done by compressor
- keep internal pressures within safe ranges

[figure from Shuki Ronen, LISS]


Quarry Data
Airgun


Tuned Pulse Source
[figure from Shuki Ronen, LISS]

Acoustic signature influenced by source volume

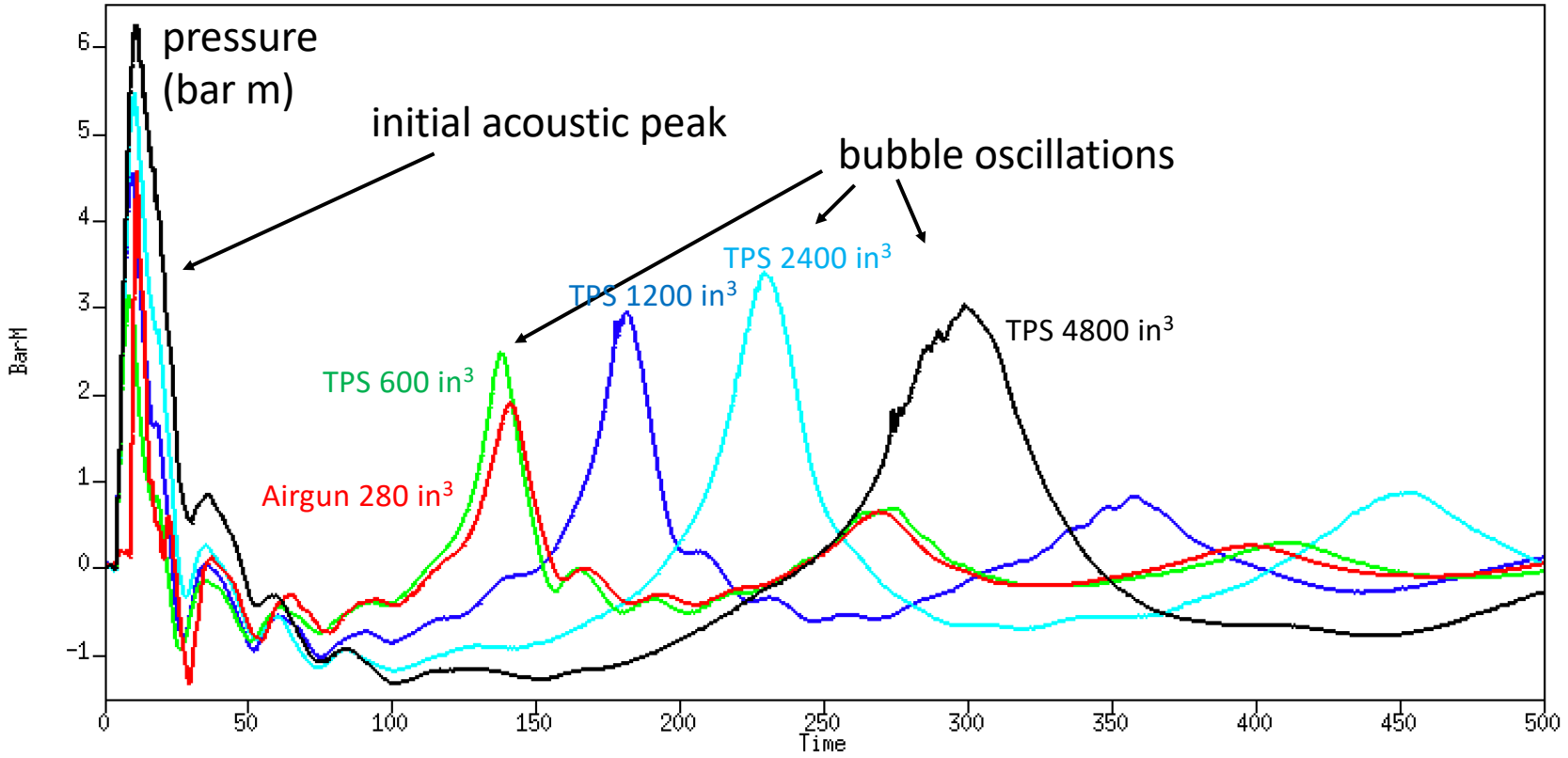

[figure from Shuki Ronen, LISS]

Zoom in on initial peak

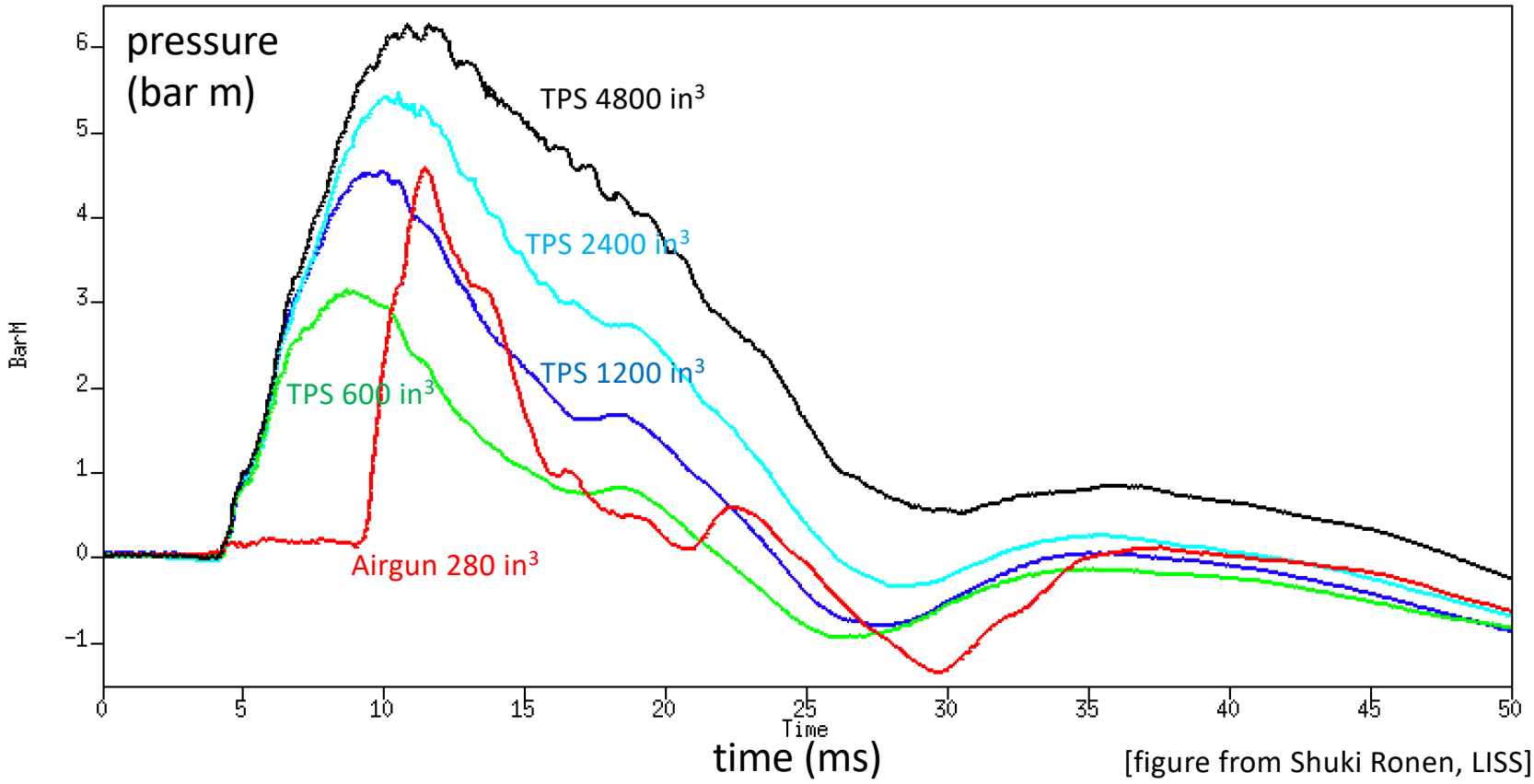

[figure from Shuki Ronen, LISS]

Large volume sources increase low frequencies

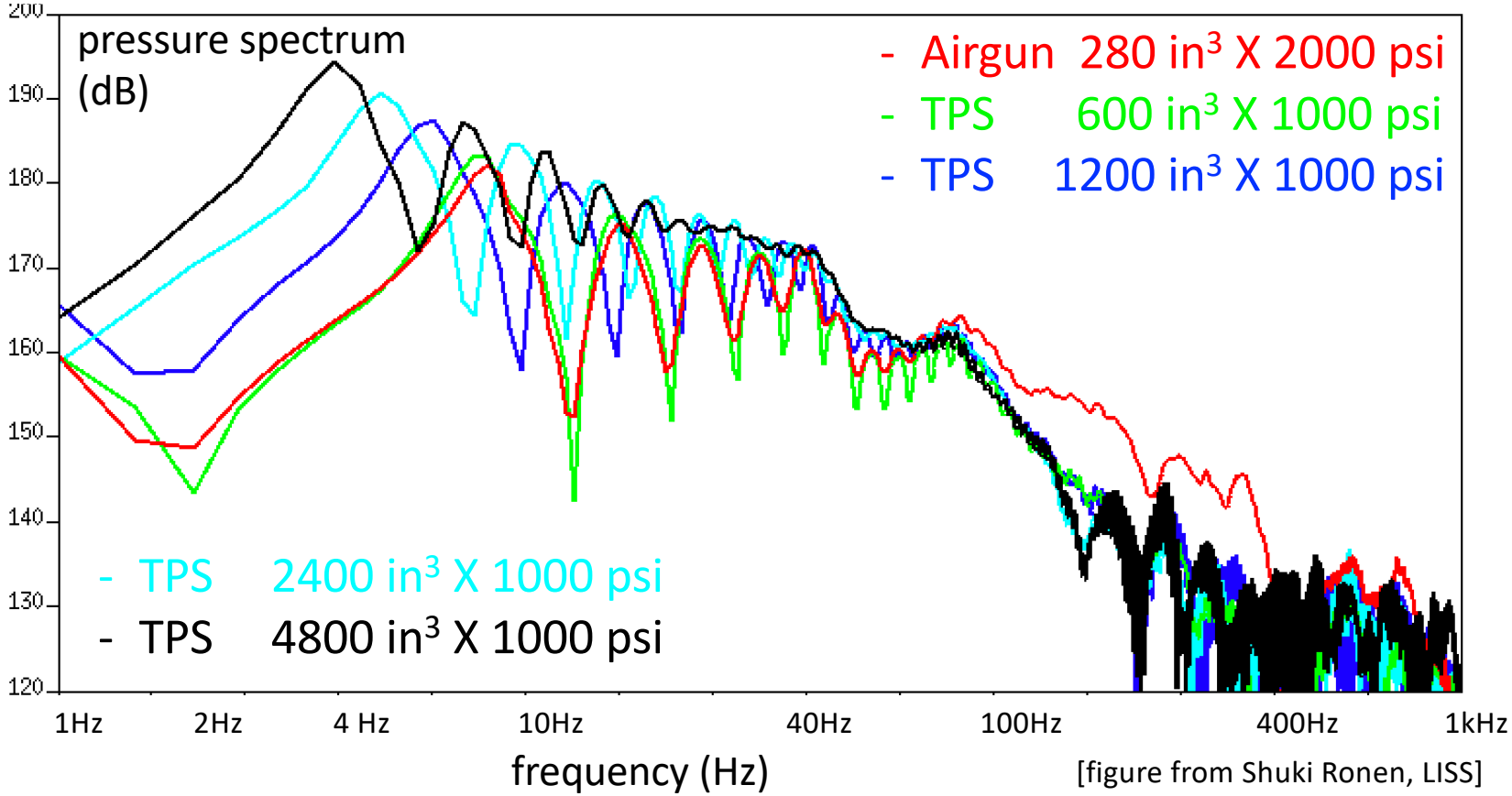

[figure from Shuki Ronen, LISS]

Source modeling

Ziolkowski [1970] applied Rayleigh-Plesset spherical bubble oscillation model

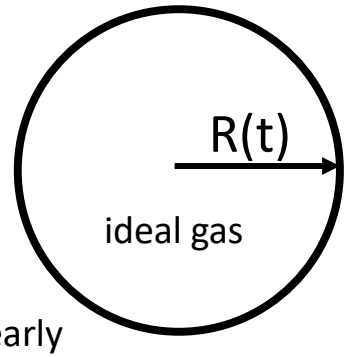

nearly incompressible water

classic approach is to *ignore source discharge process*, assuming bubble *instantly* forms with volume = source volume [e.g., Ziolkowski, 1970; Li et al., 2010; de Graaf et al., 2014]

1. water equation of motion:

imbalance of gas and water pressures

damping from acoustic radiation

$$R\ddot{R} + \frac{3}{2}\dot{R}^2 = \frac{p_b - p_\infty}{\rho_\infty} + \frac{R}{\rho_\infty c_\infty}\dot{p}_b - \alpha\dot{R},$$

inertia of water

empirical damping [Langhammer and Landrø, 1996]

2. ideal gas in bubble: $p_b = \frac{m_b Q T_b}{V_b}, \quad E_b = c_v m_b T_b.$

$$\frac{dE_b}{dt} = c_p T_a \frac{dm_b}{dt} - 4\pi M \kappa R^2 (T_b - T_\infty) - p_b \frac{dV_b}{dt},$$

3. acoustic pressure (point source solution of wave equation):

$$\Delta p(t, r) = \rho_\infty \frac{\ddot{V}_b(t - r/c_\infty)}{4\pi r}, \qquad V_b = (4/3)\pi R^3$$

Simple bubble models can accurately reproduce data from small sources

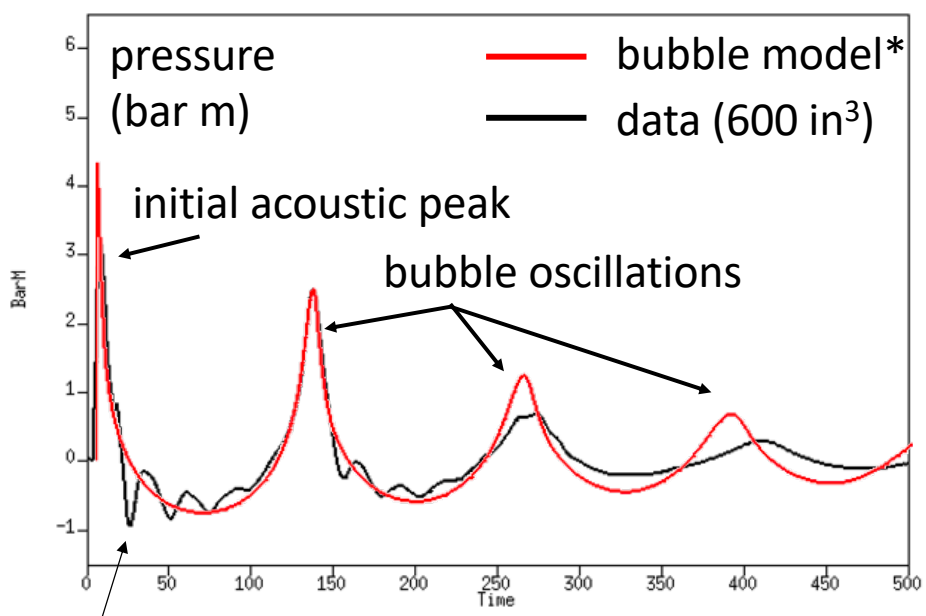

short period oscillations are reflections from quarry bottom and sides

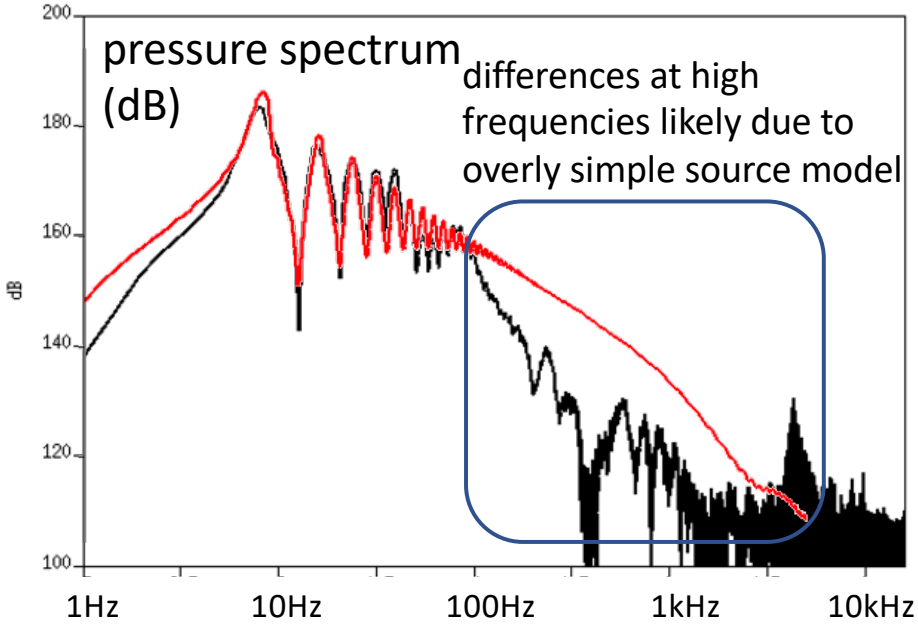

*bubble only, *instantly* forms with volume = source volume [e.g., Ziolkowski, 1970; Li et al., 2010; de Graaf et al., 2014]

[figure from Shuki Ronen, LISS]

More sophisticated modeling accounts for depressurization gas dynamics within source

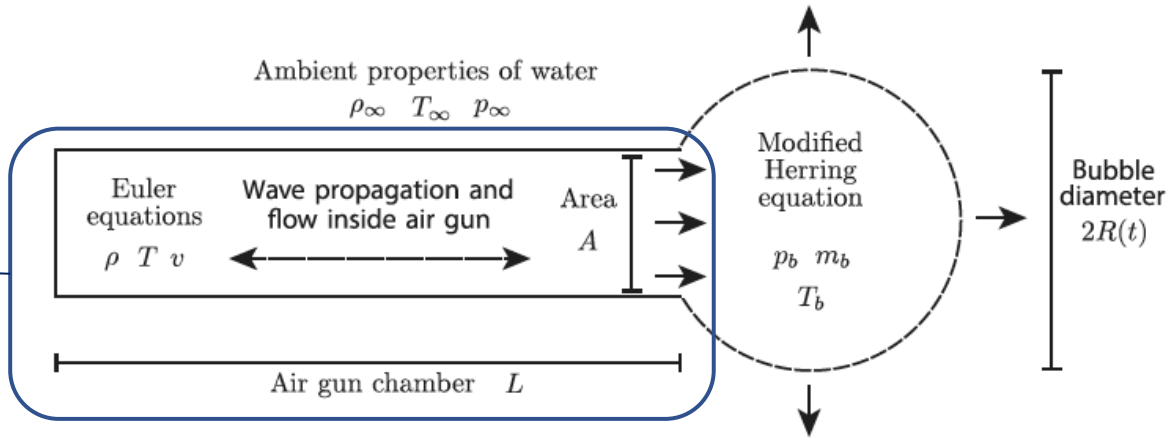

Figure 3. Schematic diagram of the coupled air-gun/bubble model.

alternative “lumped parameter” model neglects spatially variable properties within source

quasi-1D Euler equations for ideal gas

$$\frac{\partial \rho}{\partial t} + \frac{\partial (\rho v)}{\partial x} = 0,$$

$$\frac{\partial (\rho v)}{\partial t} + \frac{\partial (\rho v^2 + p)}{\partial x} = 0,$$

$$\frac{\partial e}{\partial t} + \frac{\partial [(e + p)v]}{\partial x} = 0,$$

$$p = (\gamma - 1)\left(e - \frac{1}{2}\rho v^2\right)$$

$$e = c_v \rho T$$

[Watson et al., 2019]

Depressurization gas dynamics

rarefaction travels back from port, reflects from far end

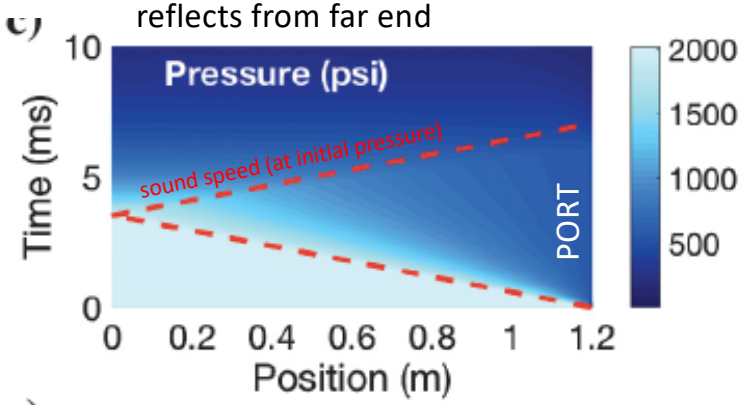

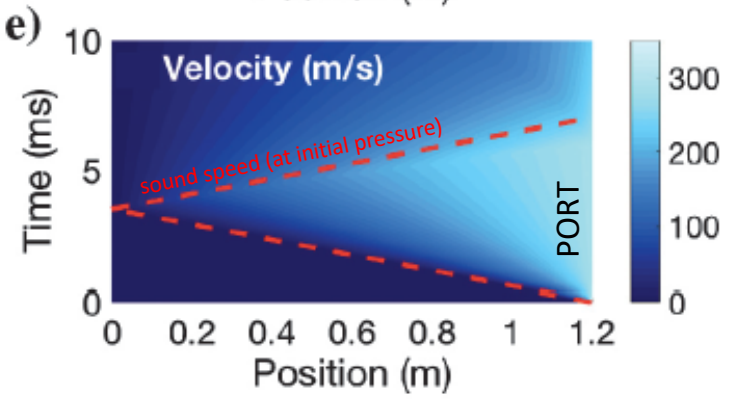

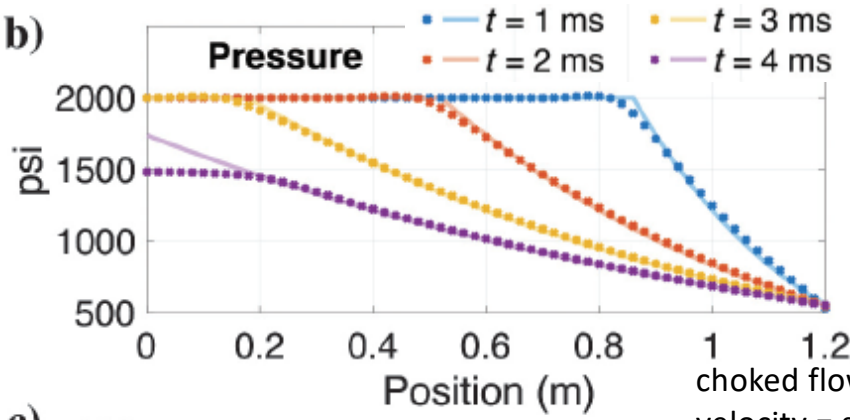

choked flow (particle velocity = sound speed)

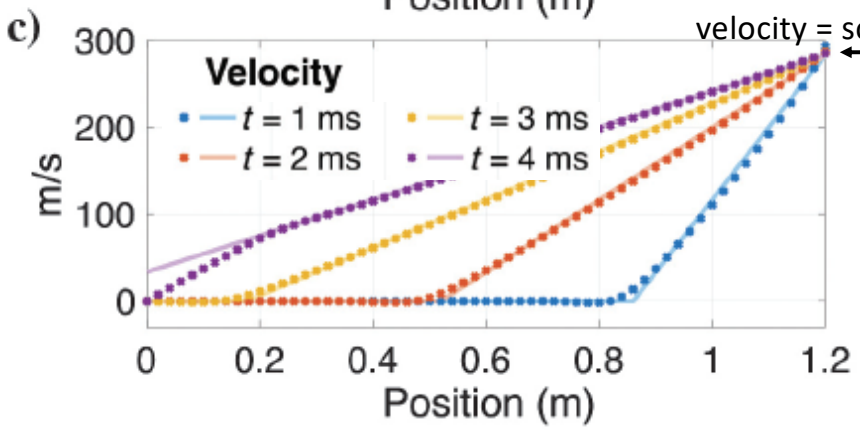

[Watson et al., 2019]

Depressurization gas dynamics influences initial acoustic peak and frequency content

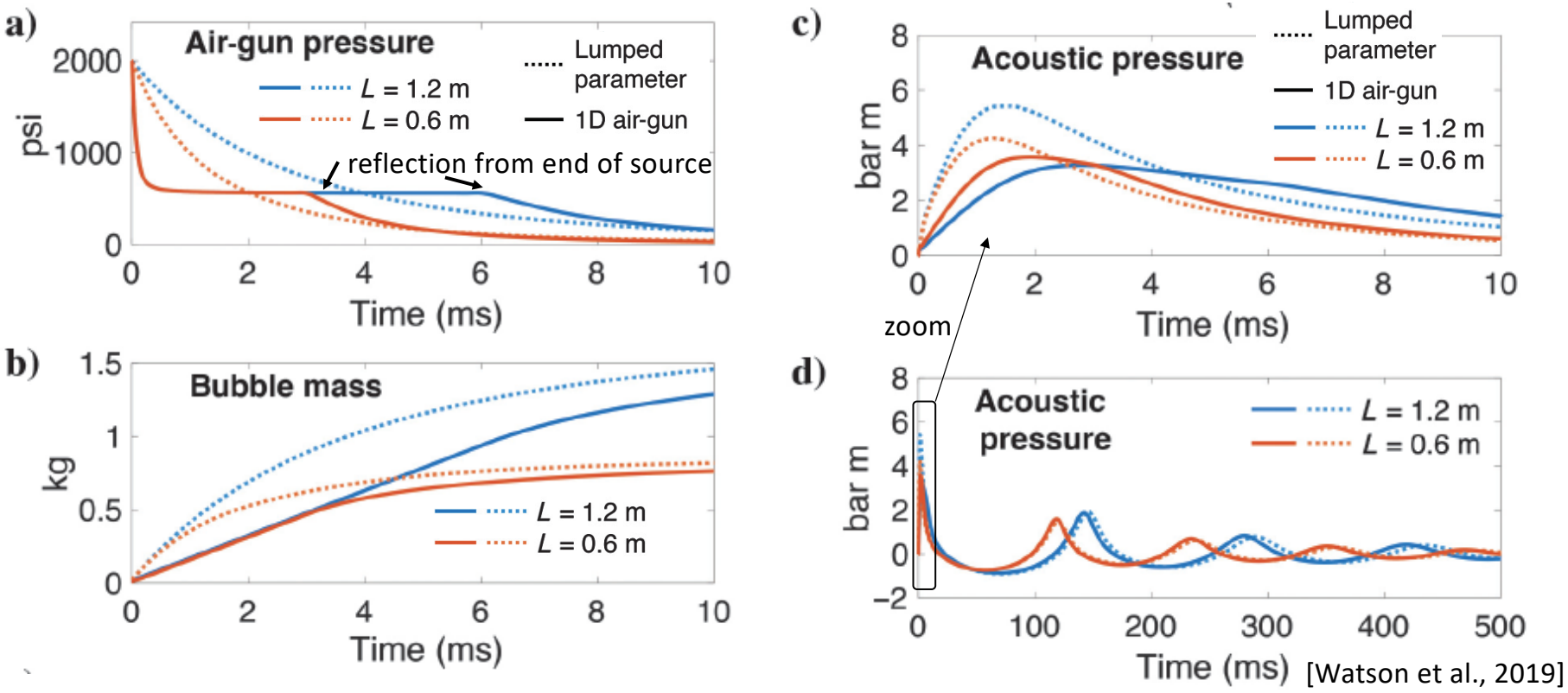

[Watson et al., 2019]

Coupled model can be ***validated*** and used to quantify ***influence of source design parameters***

validation against Seneca Lake data

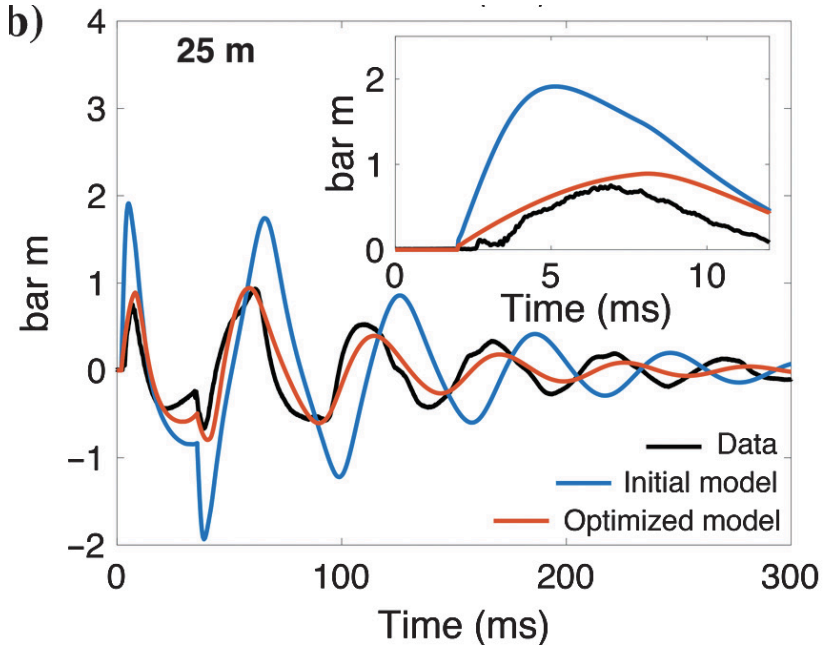

initial pressure in source

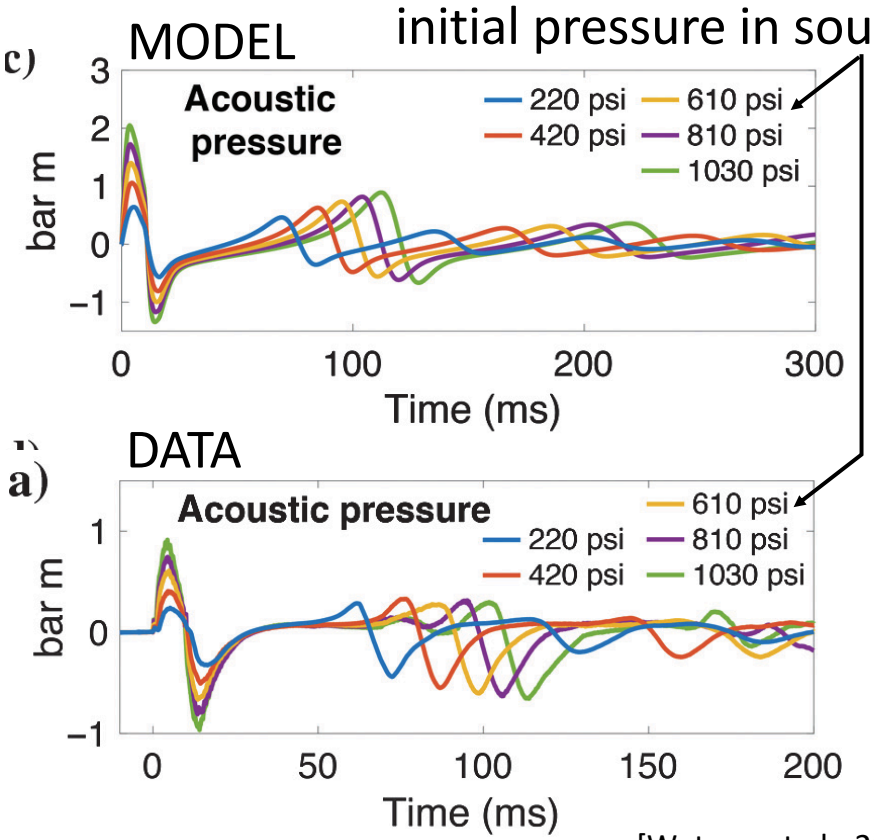

[Watson et al., 2019]

Depressurization dynamics will be essential to consider for long sources

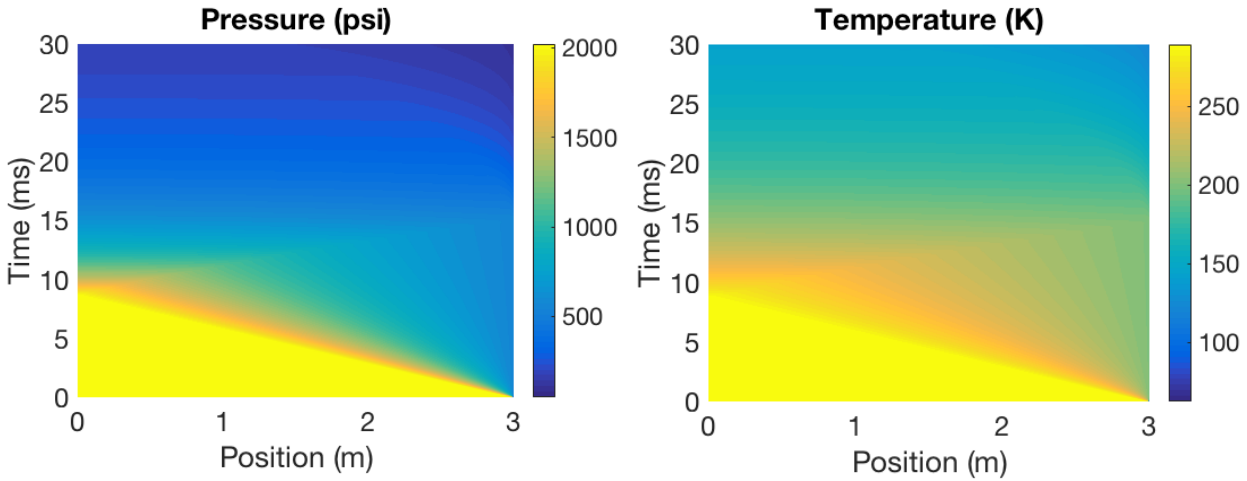

[figure from Shuki Ronen, LISS]

and there are additional challenges related to complex source design and operation!

Additional challenges: multiple chambers separated by moving shuttle that opens port

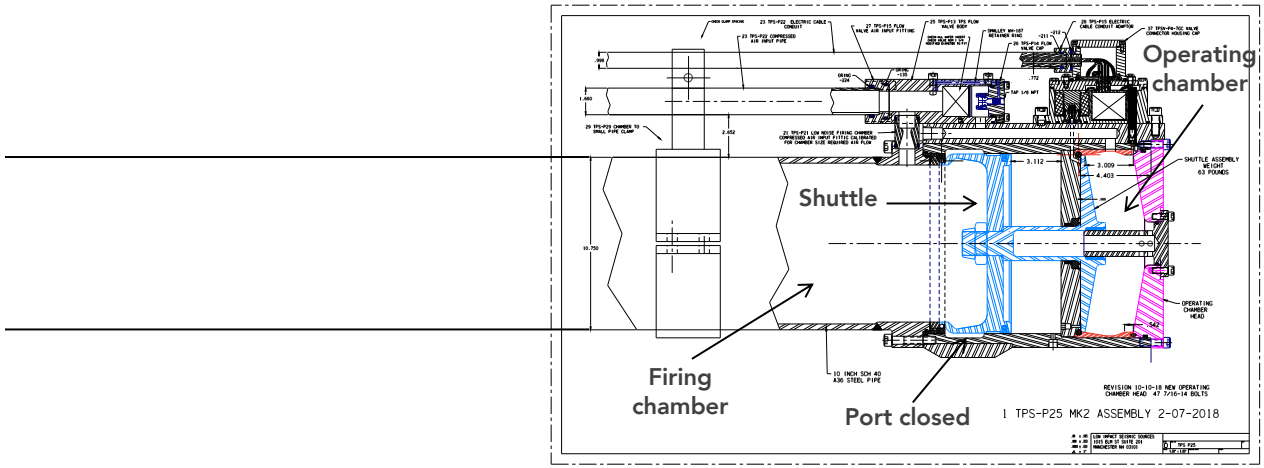

[figure from Shuki Ronen, LISS]

Additional challenges: multiple chambers separated by moving shuttle that opens port

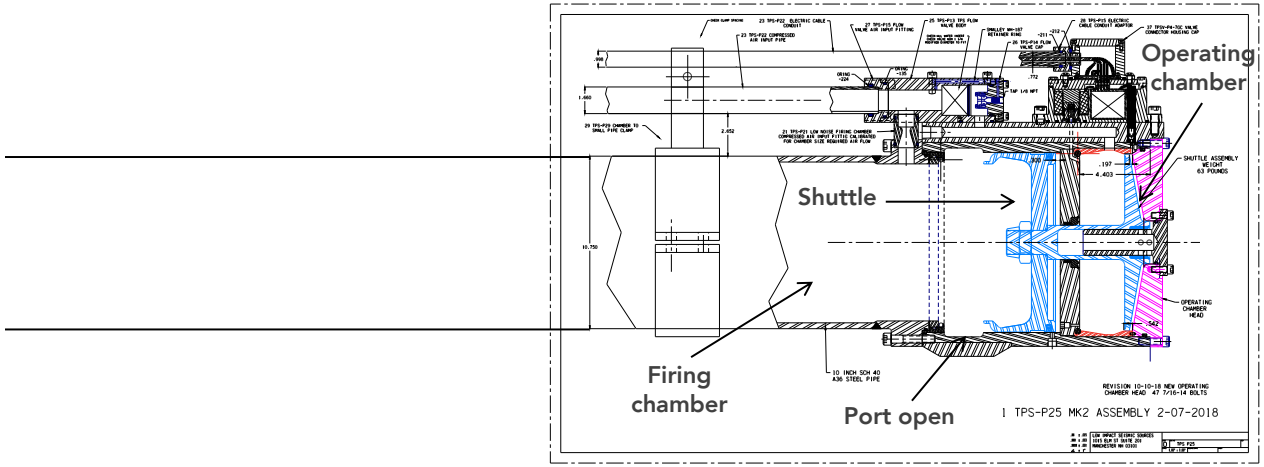

[figure from Shuki Ronen, LISS]

solution: solve Euler equations in each chamber (with moving boundaries) together with shuttle equation of motion (Newton's second law):

$$m\frac{d^2x_{shuttle}}{dt^2} = p^-A^- - p^+A^+$$

and mass conservation "interface" conditions across shuttle

Simulations accounting for moving shuttle

Solve PDEs using finite differences with time-dependent mapping

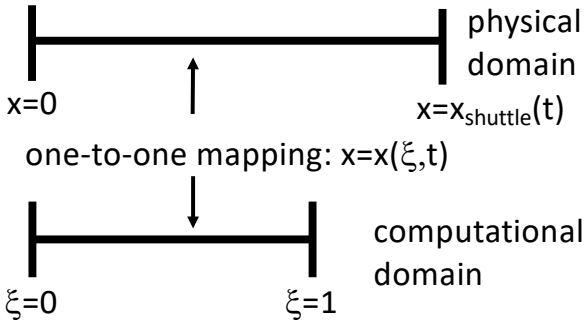

Computationally efficient alternative to 3D CFD (that can take 12 hours to several weeks per simulation [e.g., Groenaas et al., 2016])

collaboration with Uppsala University, Sweden: Ludvig Lindeberg, Ylva Rydin, Ken Mattsson, Jonatan Werpers, and Leighton Watson

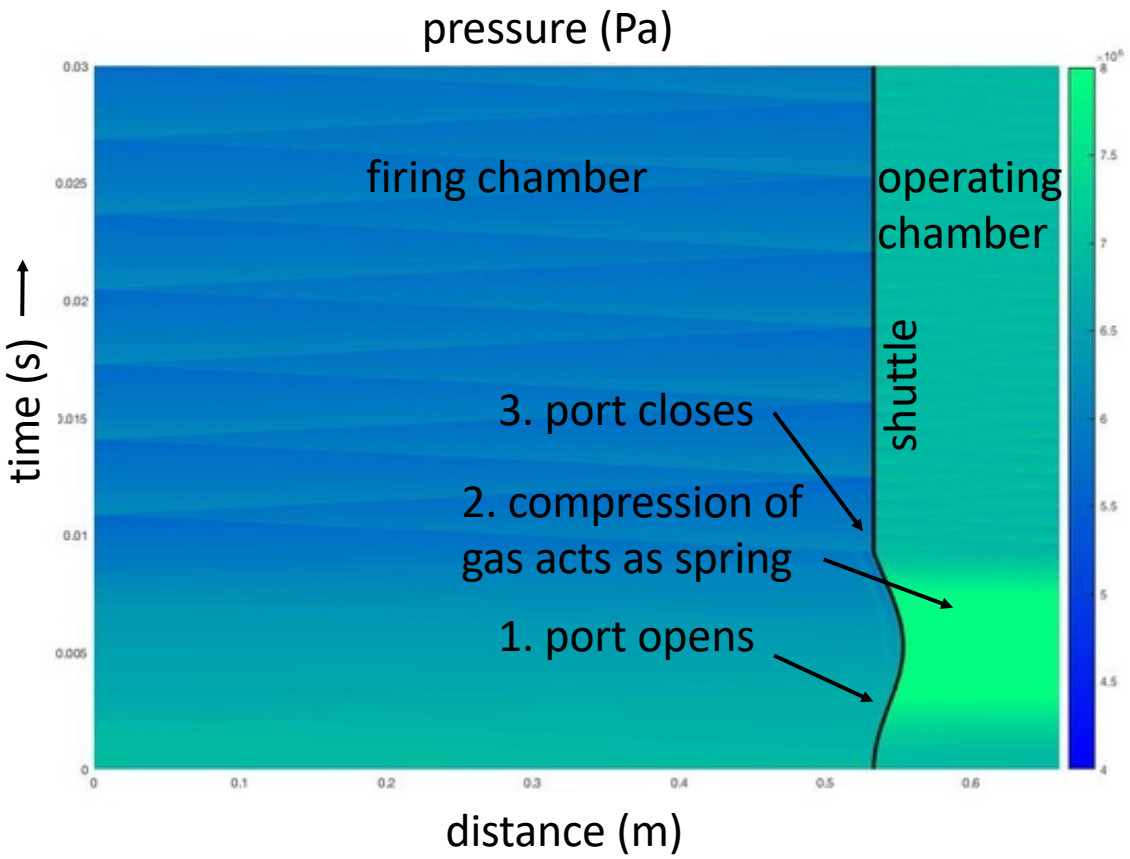

Proposed next steps for marine source modeling

- Coupling moving shuttle Euler code to our bubble code
- Switching from Matlab prototype to C++ (open source code)
- Validation by comparison to pressure and temperature data in firing and operating chambers (tests by LISS and Shell last year and this year); data shown at EAGE 2019
- Evaluation of proposed source designs using forward modeling
- Adjoint-based optimization (simulation time < minute); could be used for
  - improving source design (frequency content, radiation efficiency, etc.)
  - designaturing (especially when using Kalman filter or similar data assimilation technique to incorporate near-field hydrophone data)
- Extension from one spherically symmetric bubble to aspherical, interacting bubbles (source arrays) and moving free surface using boundary element solver

Forward and Adjoint Wave Propagation

wave propagation is central to imaging and inversion,
dominated by ***finite differences on structured meshes*** due to
superior dispersion/accuracy and computational efficiency

three challenges to which my group's work on high-order finite difference methods might contribute:

- rigorous treatment of ***interfaces*** (e.g., seafloor), with receivers and (adjoint) sources on interface
- simple procedure for ***adjoint of fully discrete problem*** (that is stable and high-order-accurate approximation to continuous adjoint problem)
- ***free surface*** and surface waves with ***topography*** (land data)

Discrete adjoints and dual consistency

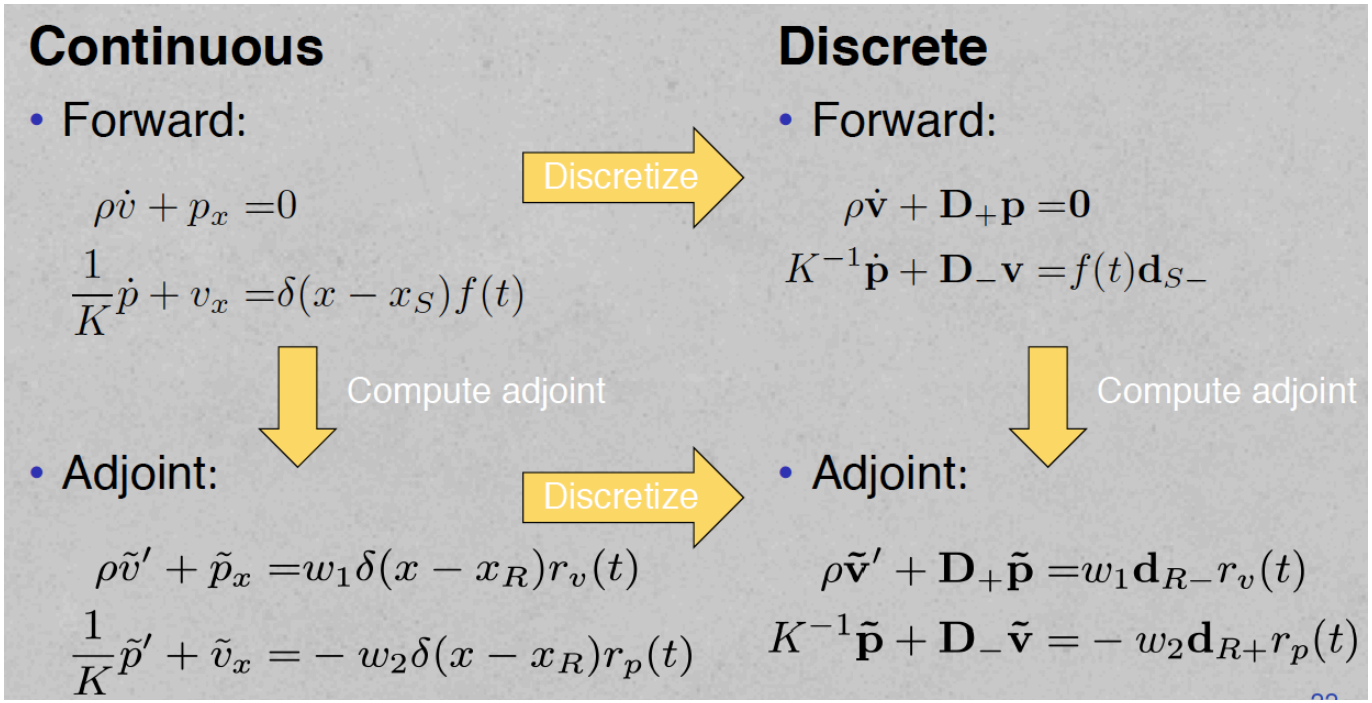

Adjoint of high-order discretization of forward problem is generally ***not*** high-order discretization of continuous adjoint problem. Methods with this property are ***dual consistent*** [e.g., Berg and Nordstrom, 2013; Hicken and Zingg, 2014]

[schematic from Joe Jennings, 1D acoustics on staggered grid]

We've now developed dual consistent schemes for FWI problems using both

1. velocity-stress (first-order hyperbolic system) staggered grid finite differences
2. displacement or velocity potential (second-order wave equation) finite differences.

Acoustic-Elastic Coupling

both acoustic and elastic solved using
second-order form of wave equation

INTERFACE BETWEEN TWO
FINITE DIFFERENCE MESHES

ACOUSTIC WAVE EQUATION
USING VELOCITY POTENTIAL

$$\rho\ddot{\phi} = K\partial_j\partial_j\phi$$

both valid for spatially
variable properties

ELASTIC WAVE EQUATION
USING DISPLACEMENTS

$$\rho\ddot{u}_i = \partial_i\lambda\partial_j u_j + \partial_j\mu\partial_i u_j + \partial_j\mu\partial_j u_i$$

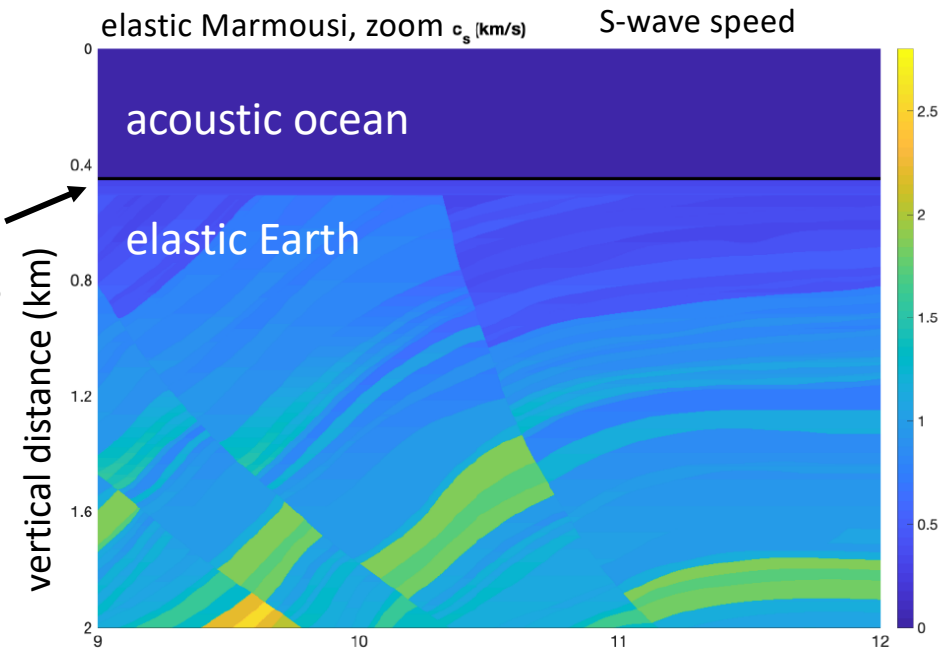

summation-by-parts finite differences:

- standard central difference operators away from boundaries/interfaces
- special one-sided difference operators near boundaries/interfaces
- built-in quadrature operators (useful for sensitivity kernels / gradients in FWI)
- provably stable methods for enforcing boundary/interface conditions
- high-order accurate (e.g., 6^{th} order interior, 3^{th} order boundary, 5^{th} order global)

[Mattsson and Nordstrom, 2004; Mattsson, 2012; Virta and Mattsson, 2014; Duru and Virta, 2014; Petersson and Sjogreen, 2015]

Source-receiver dual consistency

Data in FWI are time series at point; predicted values extracted from solution using ***receiver restriction operator*** (e.g., nearest grid point).

Adjoint source is residual time series injected at receiver location, using ***point source operator*** (e.g., nearest grid point).

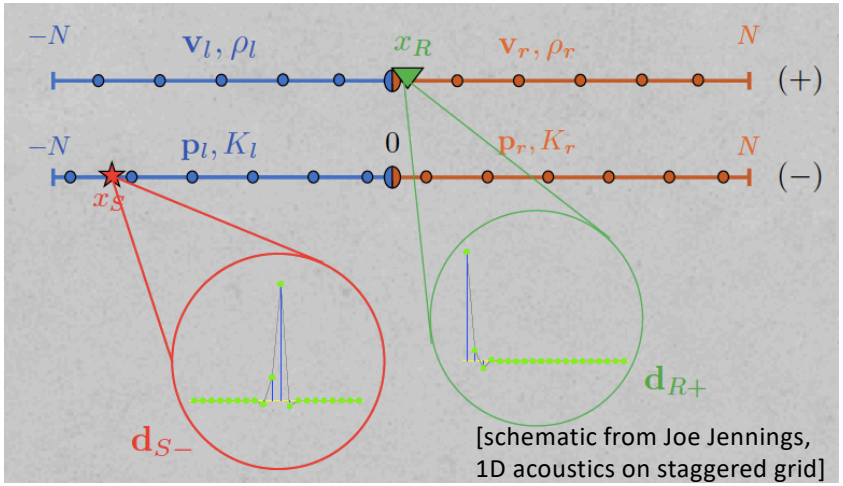

High-order discretizations of delta function, even for sources between grid points [Walden, 1999; Petersson et al., 2016]

Use of high-order discretization for adjoint source requires ***dual-consistent receiver restriction operator*** in forward simulation.

(and with this, and certain time-stepping methods, fully discrete scheme is self-adjoint* → same code for forward and adjoint problems)

*more complicated for staggered grid… though same code can still be used if boundary/interfaces are handled in special manner

Seafloor (adjoint) sources

rumors of work-arounds for sources on fluid or solid side of seafloor (shifting source or interface or even adjusting source type) → artifacts in adjoint wavefield → artifacts in gradient → artifacts in image

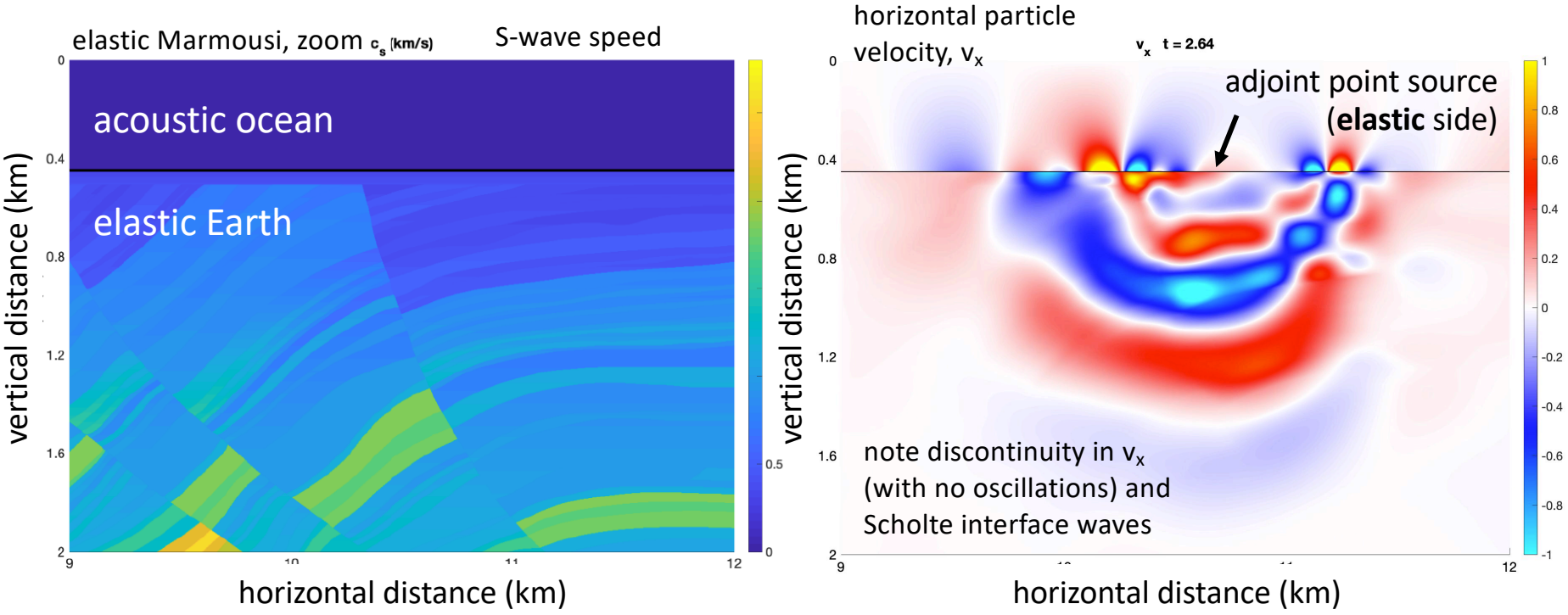

[simulations by Martin Almquist]

Seafloor (adjoint) sources

rumors of work-arounds for sources on fluid or solid side of seafloor (shifting source or interface or even adjusting source type) → artifacts in adjoint wavefield → artifacts in gradient → artifacts in image

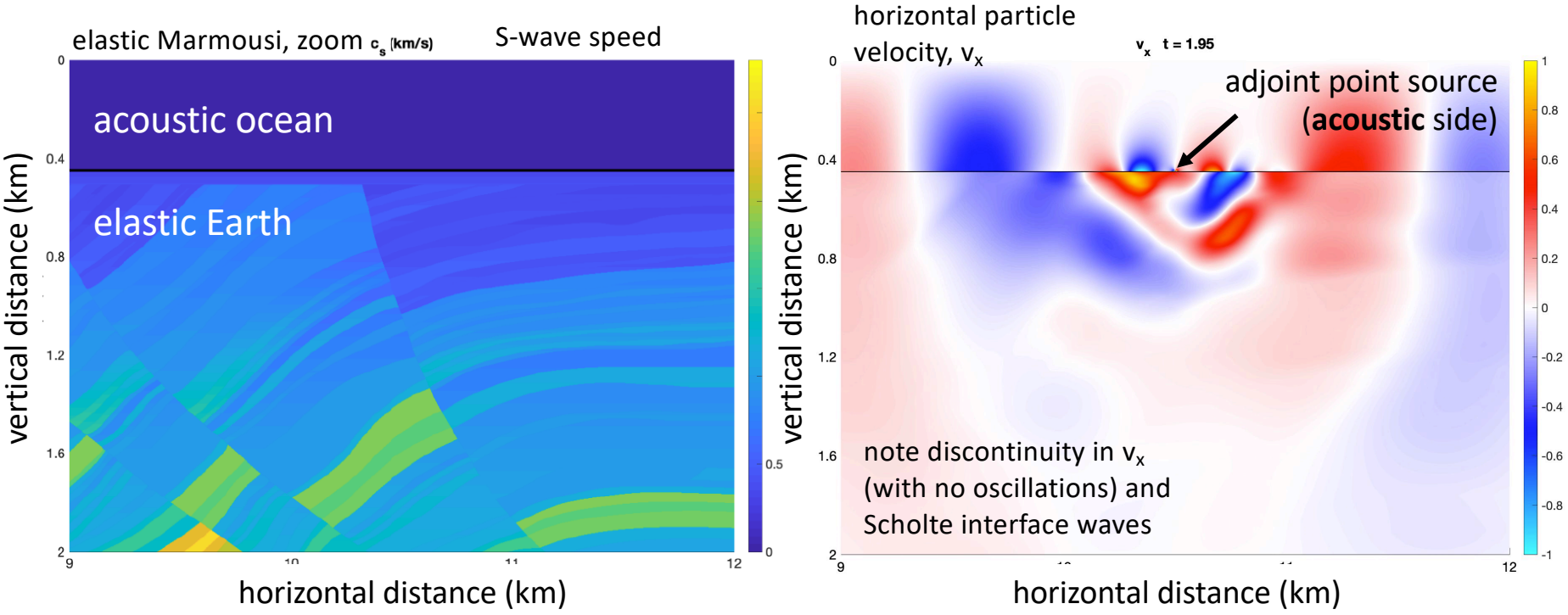

[simulations by Martin Almquist]

Surface waves, topography, and land data

imaging with land data is notoriously difficult

- methods like discontinuous Galerkin or spectral elements are ideal, from numerical perspective, but are far less efficient than finite differences
- finite differences for elastic wave equation in second-order (displacement) form are typically restricted to 2nd order accuracy, Cartesian meshes, and sometimes have stability issues near free surface—all issues that are overcome by recently developed SBP operators on curvilinear meshes

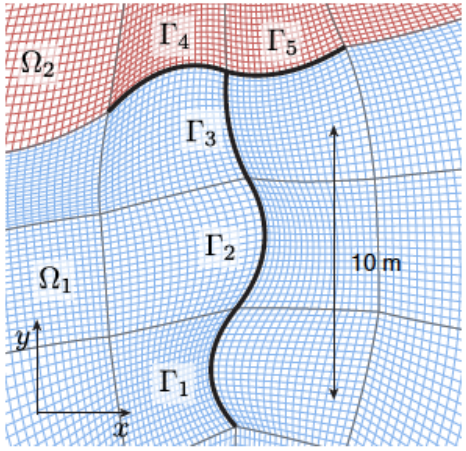

[O'Reilly et al., 2017]

curvilinear, boundary-conforming mesh in physical domain

$$a\ddot{u} = \partial_{x_i} b \partial_{x_i} u,$$

coordinate transform maps each block to unit square

$$\text{one-to-one mapping } x_i = x_i(\xi_1, ..., \xi_d)$$

topography/bathymetry enters through coefficients

$$\partial_{x_i} b \partial_{x_i} = \mathcal{K}_{ij} \partial_{\xi_j} b \mathcal{K}_{ij} \partial_{\xi_j}$$

$$\mathcal{K}_{ij} = \frac{\partial \xi_j}{\partial x_i}$$

finite differences on Cartesian mesh in computational domain

(with similar, but more complex, extension to elastic wave equation)

Convergence tests demonstrate accuracy

(and efficiency relative to existing schemes due to improved boundary treatment)

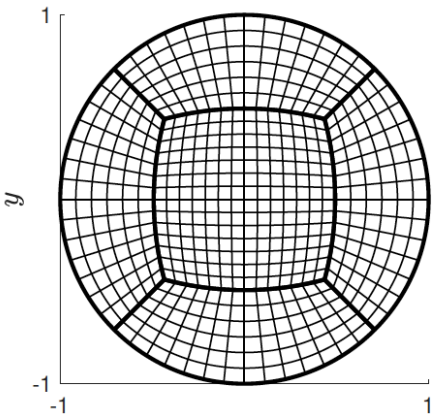

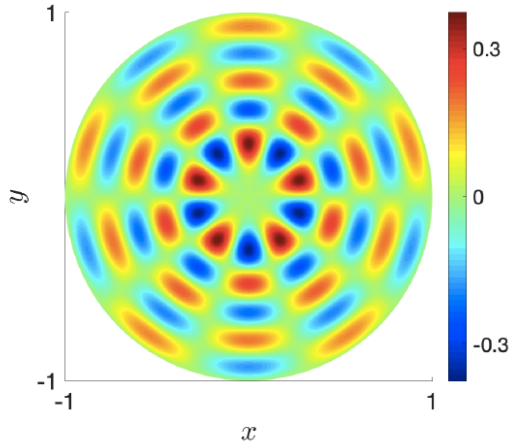

convergence tests utilize exact solution on unit disk

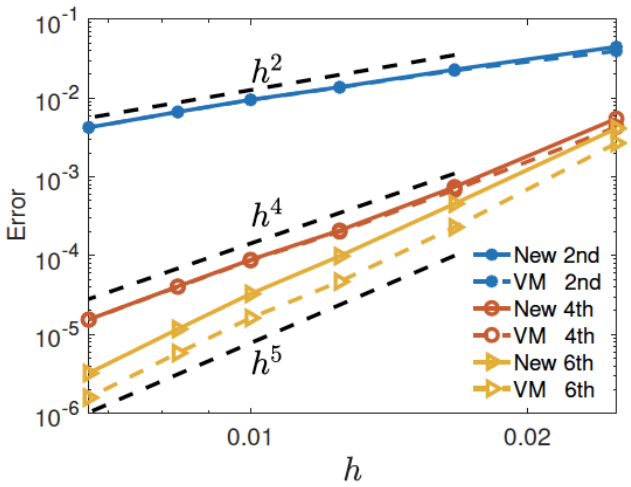

(a) Convergence rates

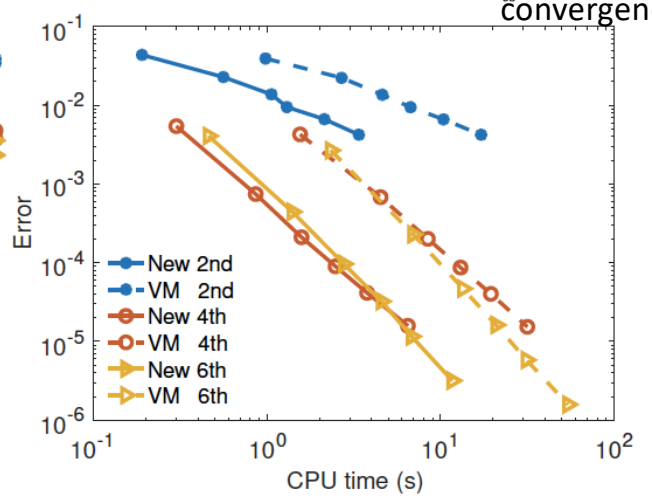

(b) Computational efficiency

Figure 4: ℓ^2 errors as functions of (a) grid spacing and (b) CPU time.

<u>boundary treatment</u>

New = our new method

VM = Virta and Mattsson, 2014

[Almquist and Dunham, 2019, in prep.]

Elastic topography example

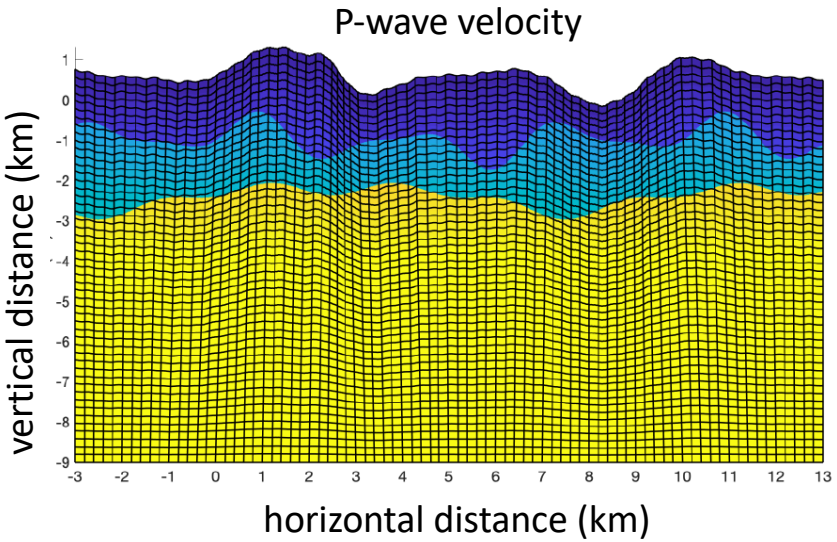

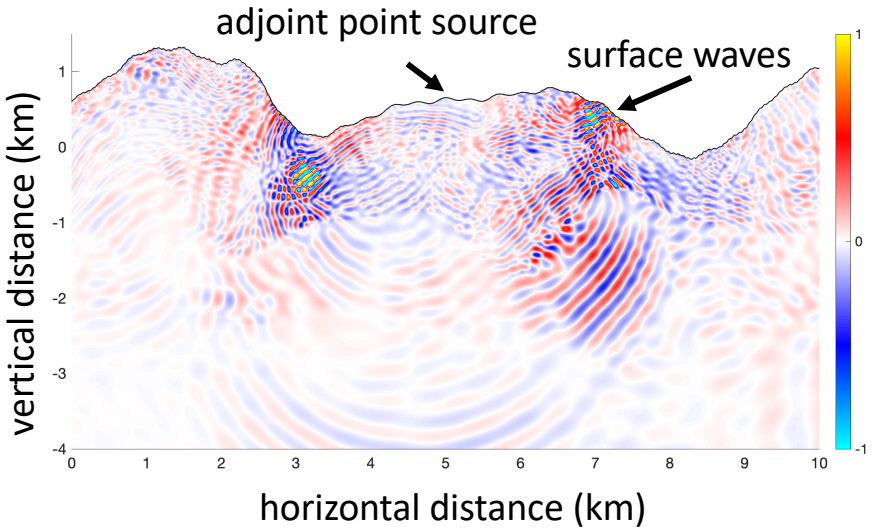

[simulations by Martin Almquist]

adjoint simulation (vertical point force on surface)
horizontal particle velocity v_x

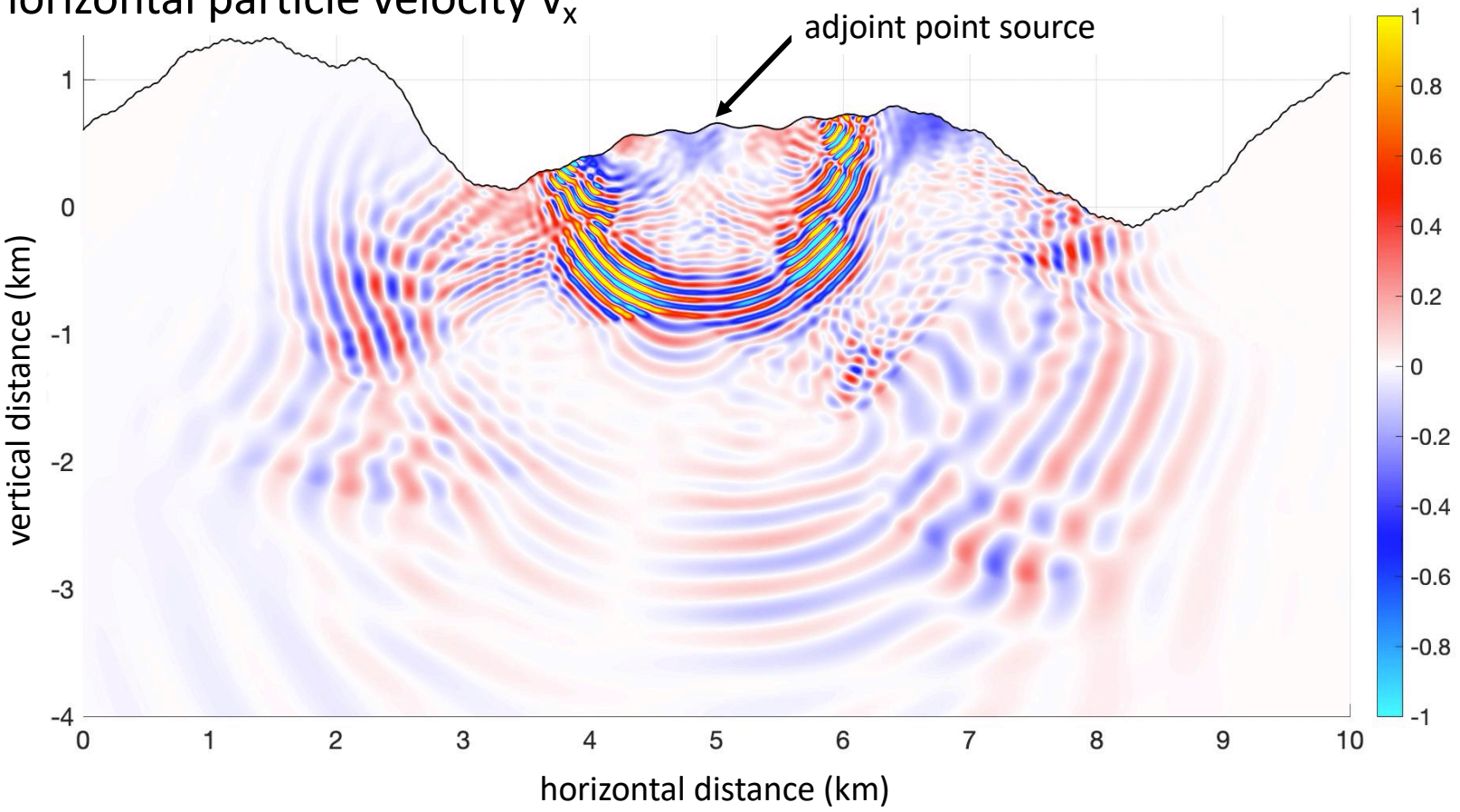

[simulations by Martin Almquist]

adjoint simulation (vertical point force on surface)
horizontal particle velocity v_x

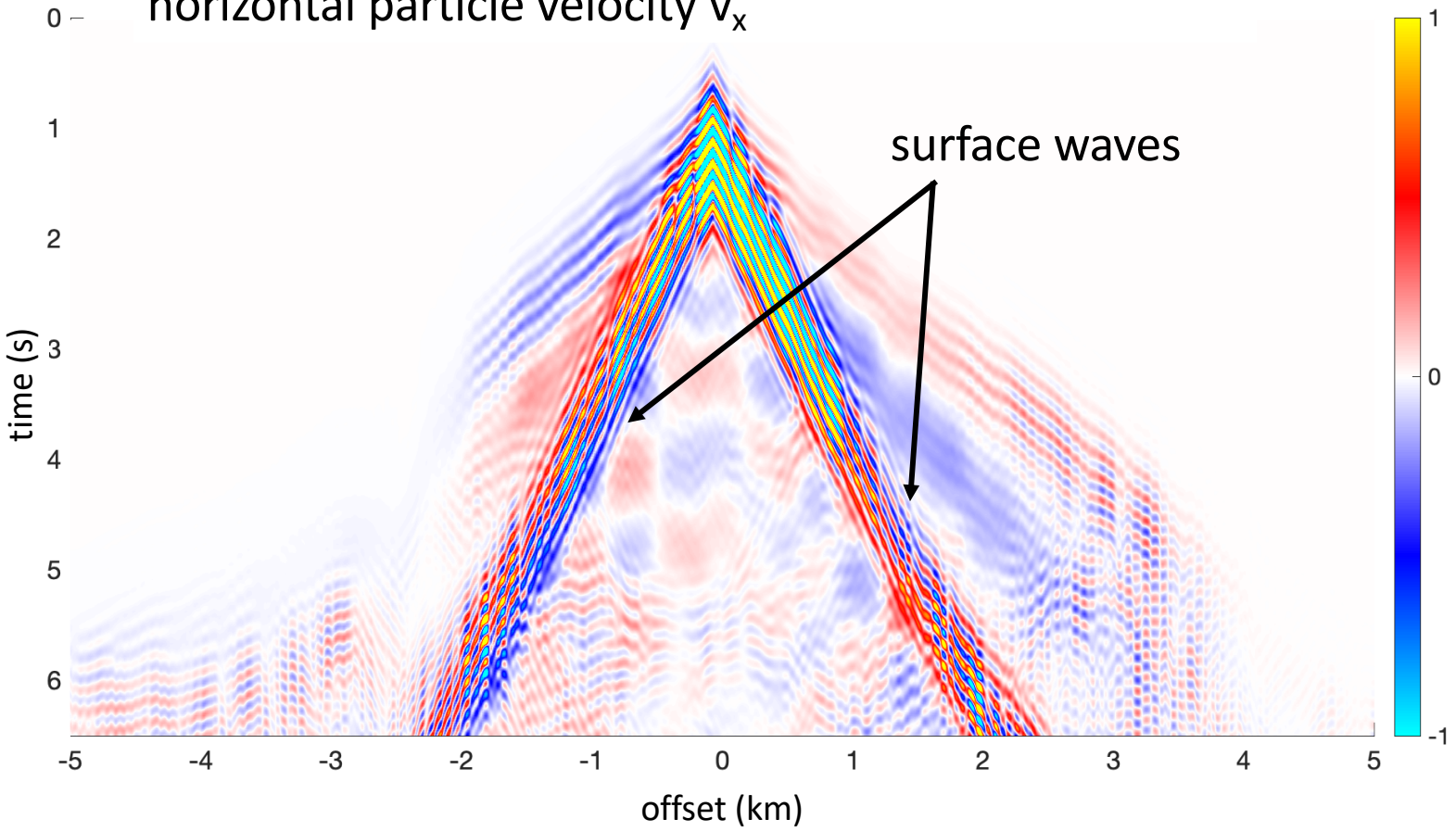

[simulations by Martin Almquist]

Proposed next steps for wave equation modeling

- 2D FWI studies to demonstrate utility of dual consistent schemes and high-order discretization of singular sources
- 3D elastic code with topography ("second project" with SEP student and my postdoc Martin Almquist)

Proposed next steps for marine source modeling

- Coupling moving shuttle Euler code to our bubble code
- Switching from Matlab prototype to C++ (open source code)
- Validation by comparison to pressure and temperature data in firing and operating chambers (tests by LISS and Shell last year and this year); data shown at EAGE 2019
- Evaluation of proposed source designs using forward modeling
- Adjoint-based optimization (simulation time < minute); could be used for
  - improving source design (frequency content, radiation efficiency, etc.)
  - designaturing (especially when using Kalman filter or similar data assimilation technique to incorporate near-field hydrophone data)
- Extension from one spherically symmetric bubble to aspherical, interacting bubbles (source arrays) and moving free surface using boundary element solver